

CHAPTER 3

Data Quality Control and Enhancement

3.1 Introduction

Characterization and evaluation of hydrocarbon reservoirs are typically achieved using a combination of all available subsurface data which is normally seismic data and well data. Main input seismic data for reservoir characterization may include pre-stack, post-stack seismic data and velocity analysis data while main well data may include logs, VSP and check-shots. Therefore, two data types should be correct for better reservoir definition and rock properties information. But if well logs data are incorrect or not completely editing, they will affect erroneous assumptions and cause many problems in the results when integrating with seismic data in interpretation tasks. Integrated interpretation of any geological model requires careful use of petrophysical logs and other well-derived data.

3.2 Well Log Quality Control, Editing and Repairing

For many reasons, well logs data often require processing, editing and normalization before they can be used for reservoir characterization. The basic well log editing workflow is in Figure 3.1. For reservoir characterization or AVO analysis, seven well logs curves are used commonly including P-wave sonic, density, S-wave sonic, Poisson's ratio, resistivity, gamma ray and SP. In these seven log curves, the first four are mandatory whereas the last three curves represent not necessarily in measurements that may be used either to define lithologic zones or in the transform relationships. Main logs data which are P-wave sonic (DT), S-wave sonic (DTS) and density (RHOB) are available in Well A. Missing log curves can often be computed with reasonable degree of certainty (Walls et al., 2004). Two major ways to compute missing logs

are through application of rock physics principles and using neural network technology.

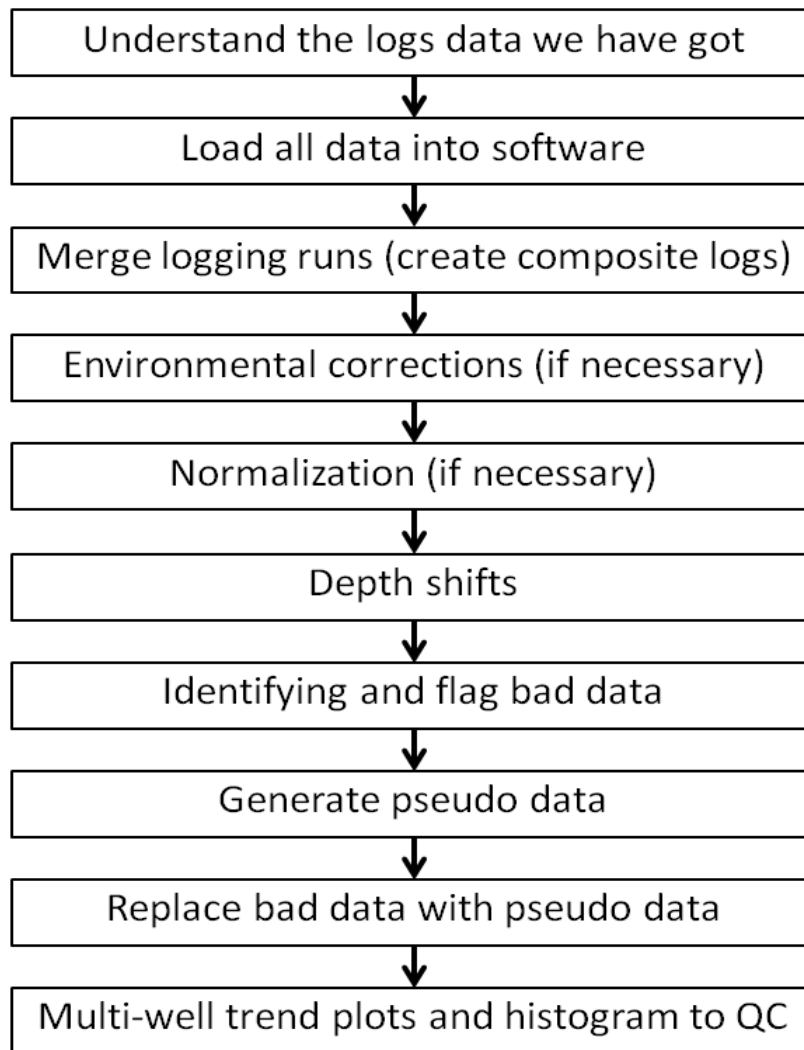


Figure 3.1: Basic well logs editing workflow.

3.2.1 Well Log Quality Control, Editing

Quality of log data is an important part of rock physics analysis and creating seismic inversion models. The petrophysicist will typically check the depth registration of various logs and make standard corrections for environmental effects on tools related to factors such as stress, mud weight, pore pressure, temperature and speed of logging (Simm and Bacon, 2014). The next step is to remove unwanted or noisy data that are from logs data especially for P-wave velocity (V_p), S-wave velocity (V_s) and RHOB (ρ). There are many different ways to check logs data and the best way is through generation of cross plots between depth, V_p , V_s and ρ etc.

a) Cross plot between depth and velocities

Vp and Vs are cross plotted to check and remove unwanted data such as spikes that have high value in velocities. The depth and Vp cross plot (Figure 3.2) shows value in depth from 2897.277 m to 4144.671 m. It shows clearly high values in the reservoir intervals which are UMA15, MMF10, MMF15 and MMF30. There is no unwanted values in depth and Vp cross plot. The depth and Vs cross plot (Figure 3.3) show values in depth from 2897.277 m to 4144.671 m. It shows high values in the reservoir intervals which are UMA15, MMF10, MMF15 and MMF30. There is no unwanted values in depth and Vs cross plot however it is recognized that missing values from 3288.03 m to 3298.393 m as shown in yellow box. The missing values in Vs will be fixed by using empirical relations in the next part of this chapter.

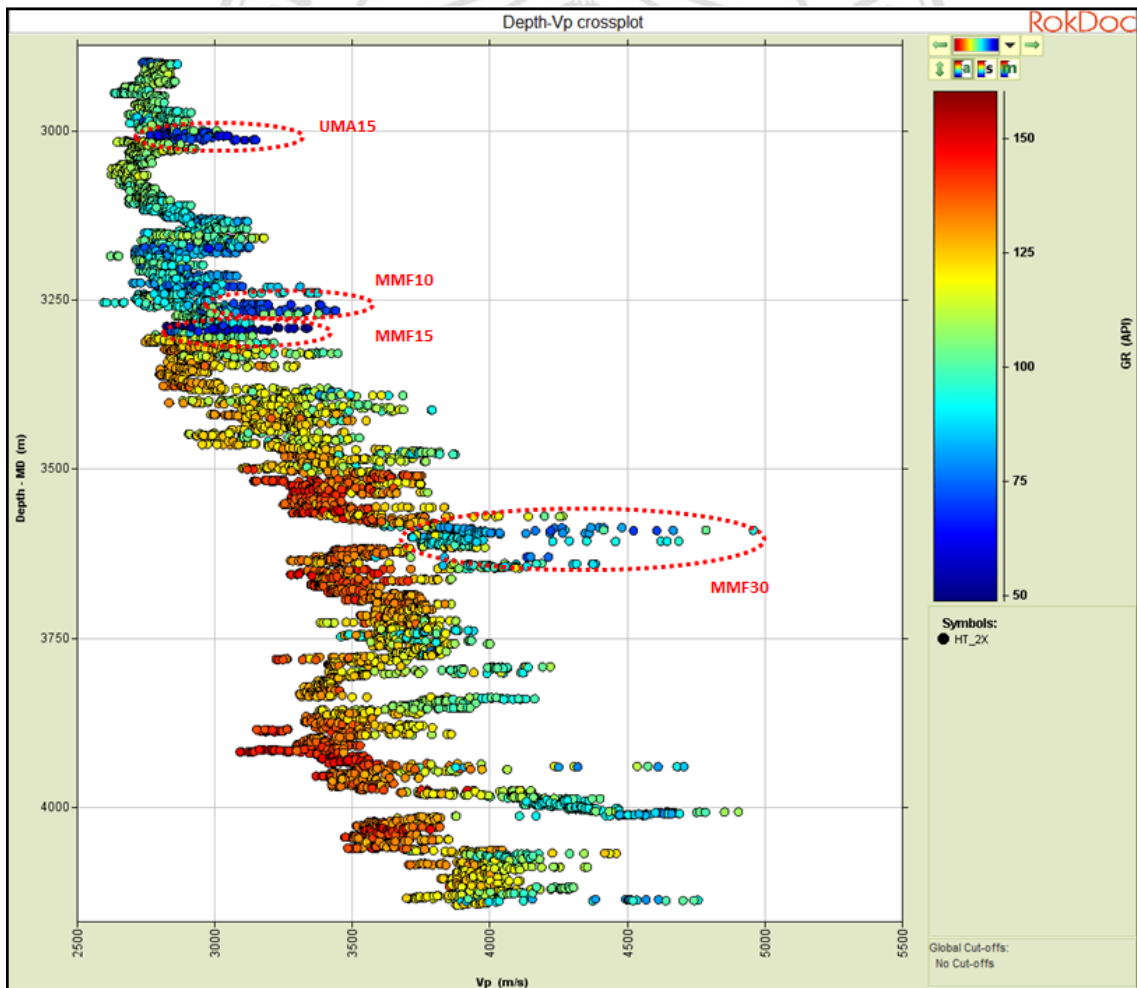


Figure 3.2: Depth and Vp cross plot. Red dashed lines zones indicate reservoir intervals.

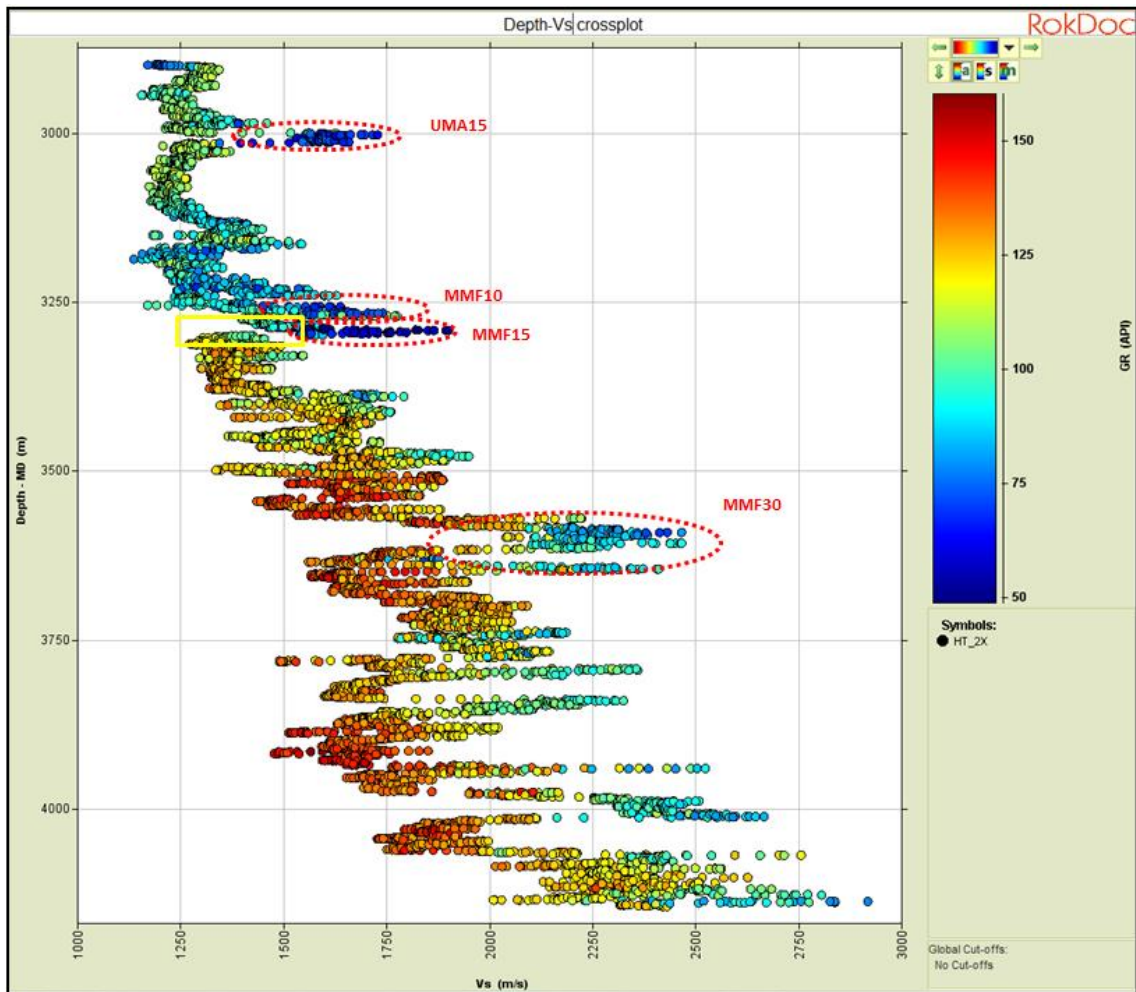


Figure 3.3: Depth and Vs cross plot. Red dashed lines zones indicate reservoir intervals. Yellow box indicates missing value data.

b) Cross plots between density and velocities

Density and velocities (V_p and V_s) data are cross plotted to find out the noisy points from log data (Figures 3.4 and 3.5). The main purpose is to remove those data that have high density but the velocities are low and vice versa. There is no noisy point from both Figure 3.4 and Figure 3.5.

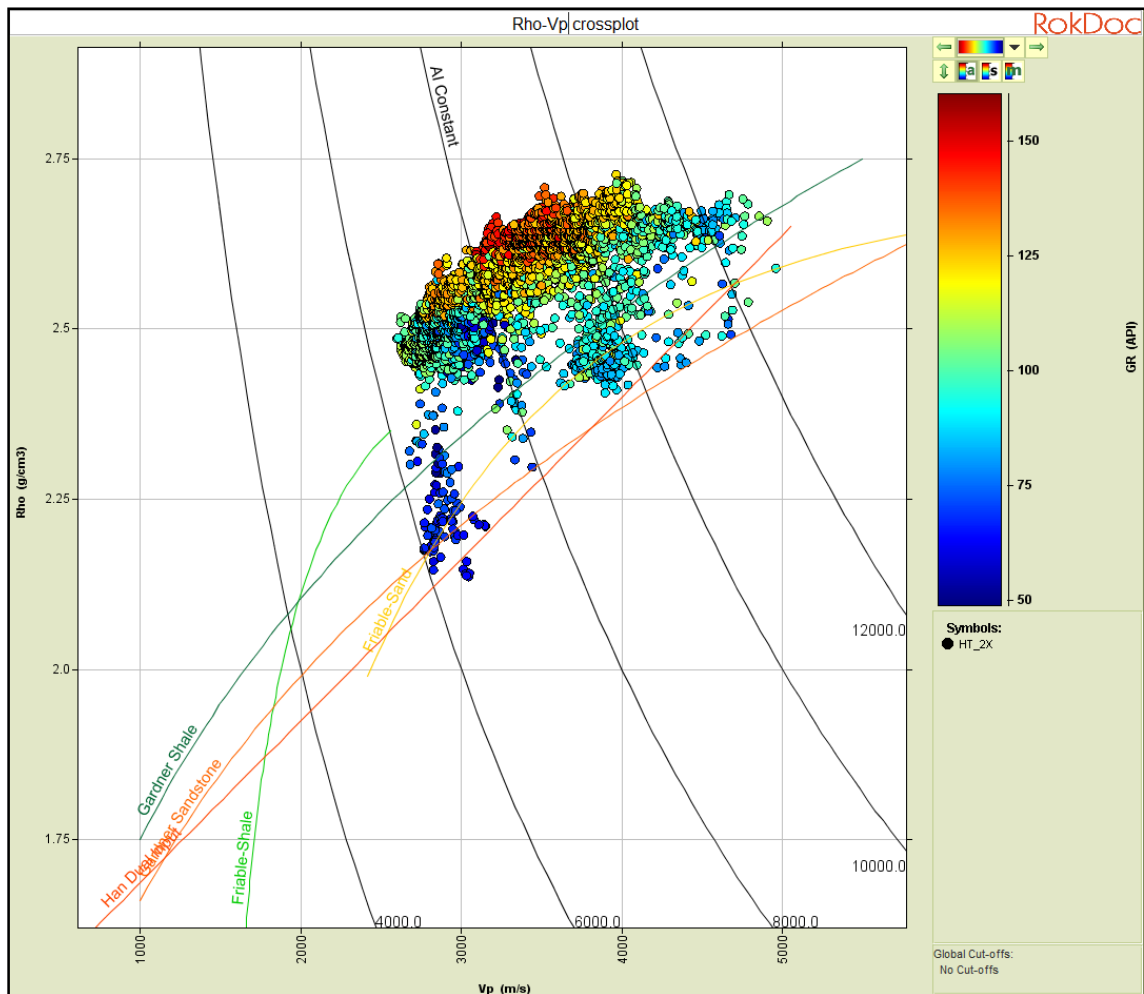


Figure 3.4: Density and Vp cross plot. The color lines represent rock physics relationships between Density and P-wave velocity found by Gardner et al., (1974).

ลิขสิทธิ์มหาวิทยาลัยเชียงใหม่
 Copyright© by Chiang Mai University
 All rights reserved

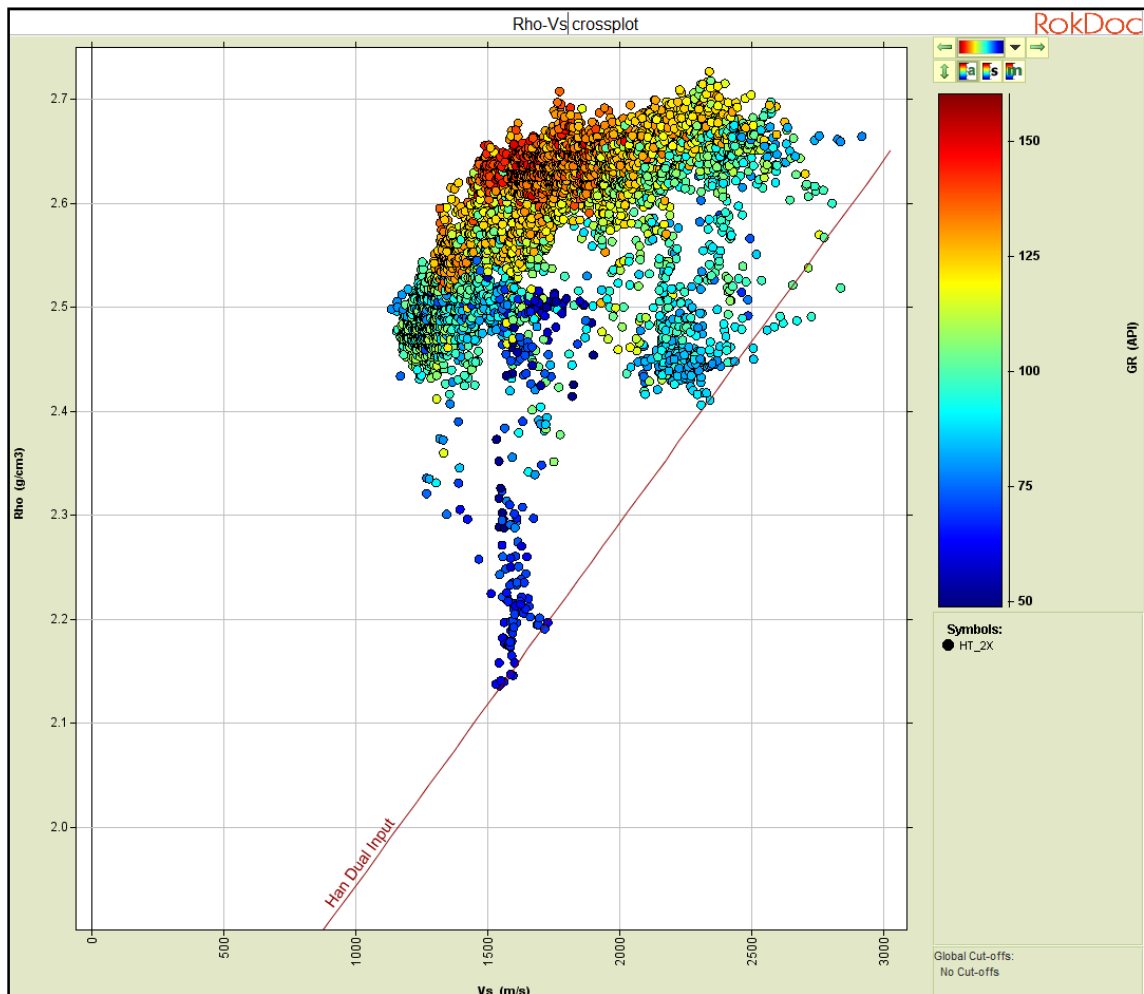


Figure 3.5: Density and Vs cross plot. The Han dual input linear line represents rock physics relationship between density (porosity) and S-wave velocity (Han et al., 1986).

ลิขสิทธิ์มหาวิทยาลัยเชียงใหม่
 Copyright© by Chiang Mai University
 All rights reserved

c) Cross plots between P-wave velocities and S-wave velocities

P-wave velocities and S-wave velocities cross plot is generated to show the best fit trends between them and to find out the wrong velocities values from the logs data. Generally, the P-wave velocities are approximately double of the S-wave velocities. Therefore, the S-wave velocities which are very high values at low values of P-wave velocities are wrong values and need to be deleted from the log data. Figure 3.6 shows cross plot of P-wave and S-wave velocities with empirical relations between compressional and shear velocities from Greenberg and Castagna (1992). It can be seen that values of P-wave velocities and S-wave velocities have similar tendency with Greenberg and Castagna relations. Main values are in the relations of Castagna mudrock and Greenberg and Castagna shale relation with high gamma ray values, while lower gamma ray values which represents brine and hydrocarbon saturation sandstone fall into Greenberg and Castagna sandstone relation and the left side of that line. Besides, the cross plot shows no wrong values of V_p and V_s .

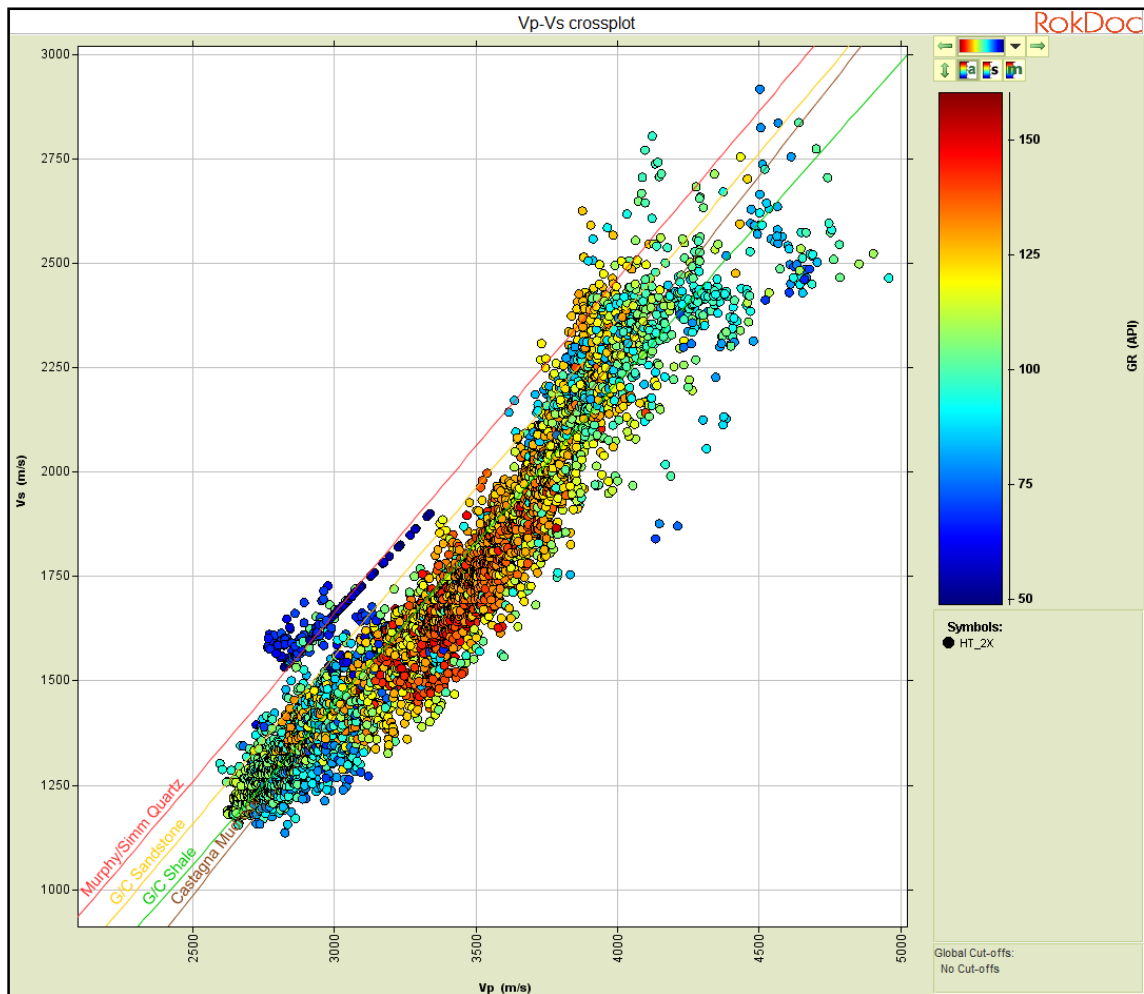


Figure 3.6: Vp and Vs cross plot with the Greenberg and Castagna Vp - Vs relations.

3.2.2 Well Log Repairing

Original well logs may require editing and correction before they are suitable for creating synthetic seismograms, rock physics models, and seismic inversion etc. There are many reasons affect the well logs causing the bad or missing data. Four main reasons are well bore washouts or casing, mud filtrate invasion, gaps or missing data and insufficient log suites. In this independent study, most of the well logs provided are good quality. However, the well logs still have some missing value which can be detected when import the well logs dataset into Hampson Russell software. In Well A, there are missing values presented in the shear wave velocity logs from 3288.03 to 3298.393 m (MD) due to casing points, position of casing shoe is 2898 mDDBRT. Casing points information is mention in final well report of Well A (Table 3.1). The

four mandatory logs for reservoir analysis are gamma ray, P-wave sonic, S-wave sonic and density logs and missing data in S-wave sonic logs are shown in Figure 3.7.

Table 3.1: Casing point from final well report.

Shoe Depth mDDBRT	Casing size	Lithology	Formation	Comments
229.0	30"		Bien Dong	Conductor.
1107.0	20"		Bien Dong	No returns, Csg set on depth.
2691.0	13-3/8"	Mudstone	Bien Dong	Set on kick tolerance
2898.0	11-3/4"	Mudstone	Bien Dong	Set on kick tolerance
3297.0	9-5/8"	Mudstone	Thong Mang Cau	Set below the Green horizon
3700.0	7"	Mudstone	Thong Mang Cau	Set after TD reached for production test

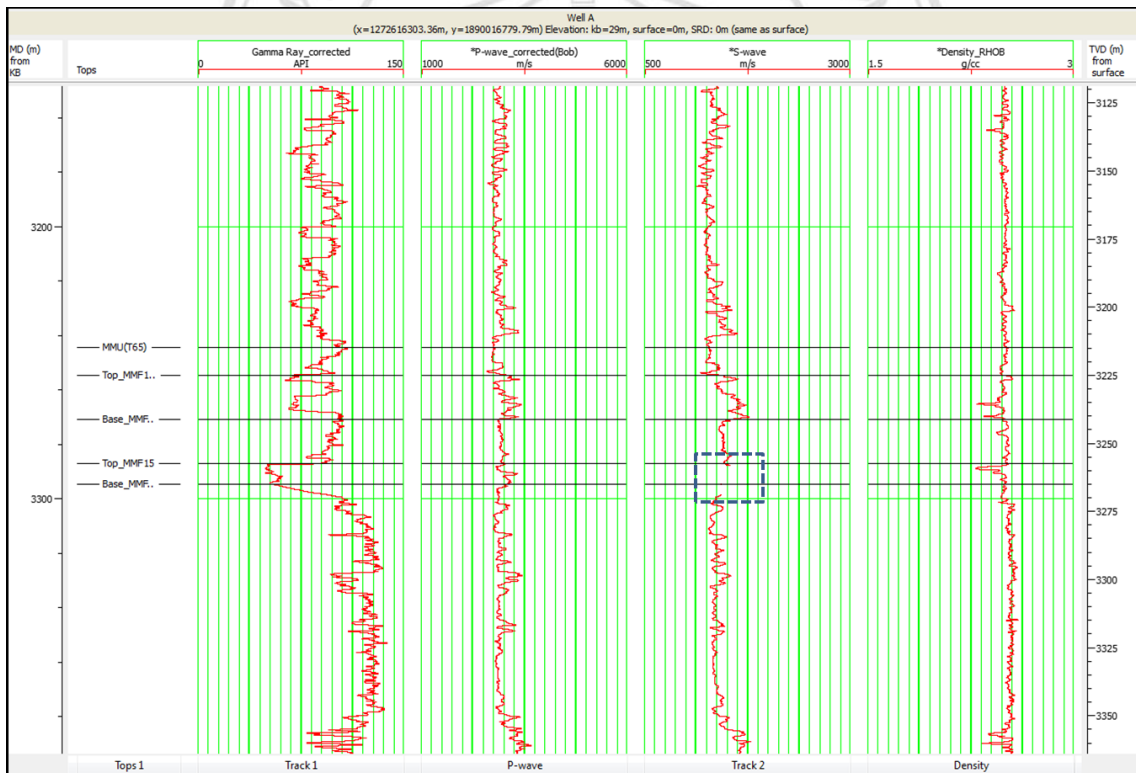


Figure 3.7: Main logs curves for reservoir characterization. Blue dashed box indicates missing data in S-wave sonic log. Formation tops T65, top and base of two sand bodies MMF10 and MMF15 are in the left hand track.

S-wave velocity log is useful for various seismic interpretation applications such as AVO analyses and quantitative interpretation. Therefore, to achieve good results in reservoir characterization analysis, it is necessary to do correction to S-wave velocity

logs. The best way for S-wave velocity estimation is through relationships between compressional and shear wave. Most of the empirical relations for P-wave and S-wave are based on Castagna et al. (1985) and Greenberg and Castagna (1992). Greenberg and Castagna (1992) empirical relations are based on a variety of dataset from the Gulf Coast and onshore United States. Experience has shown that there can be significant variations away from the Greenberg and Castagna's trends (Simm and Bacon, 2014). Therefore, those relations need modifying to use in local sedimentary basins. In this independent study, the empirical relationship between V_p and V_s is evaluated by regression analysis, the purpose of this is to find the local relationships between V_p and V_s for the Nam Con Son Basin. However, the limitation of this regression analysis is one well dataset in the basin was used. If there are many wells data available, the localized relations will be more correct.

Greenberg and Castagna (1992) defined four main trends common lithologies for sandstone, limestones, dolomite and shale. So it is essential to predict V_s from V_p depending on lithologies variations throughout Well A's depth. As shown in Figure 3.9, missing data from V_s log are from 3288.03 to 3298.393 m (MD), this interval is mainly in depth of sand dominant body. Thus, fixing the V_s missing data is estimated using localized $V_p - V_s$ relations for sandstone. First step of the regression analysis is cross plotting the V_p versus V_s to obtain the linear regression for the sandstone. In Well A, there are four main intervals that have sandstone dominantly in lithologies: UMA15, MMF10, MMF15 and MMF30. Those intervals are defined using top and base that provided by the company. Therefore, V_p and V_s in UMA15, MMF10 and MMF30 sandstone intervals are cross plotted separately to find relations between V_p - V_s for each intervals. Cross plots of UMA15, MMF10 and MMF30 intervals are in Figures 3.8 to 3.10 respectively. The linear relationship between V_p and V_s is also showed for each intervals.

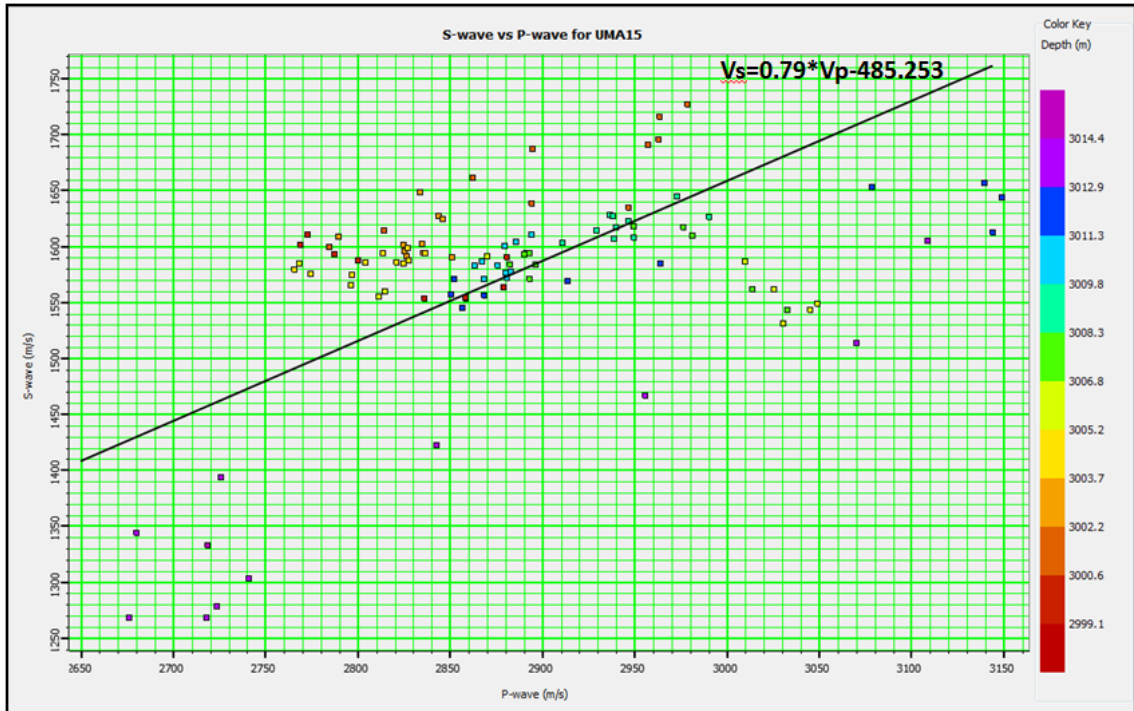


Figure 3.8: Cross plot V_s and V_p for UMA15. Linear relationship between V_s and V_p is defined by equation $V_s = 0.79 * V_p - 485.253$.

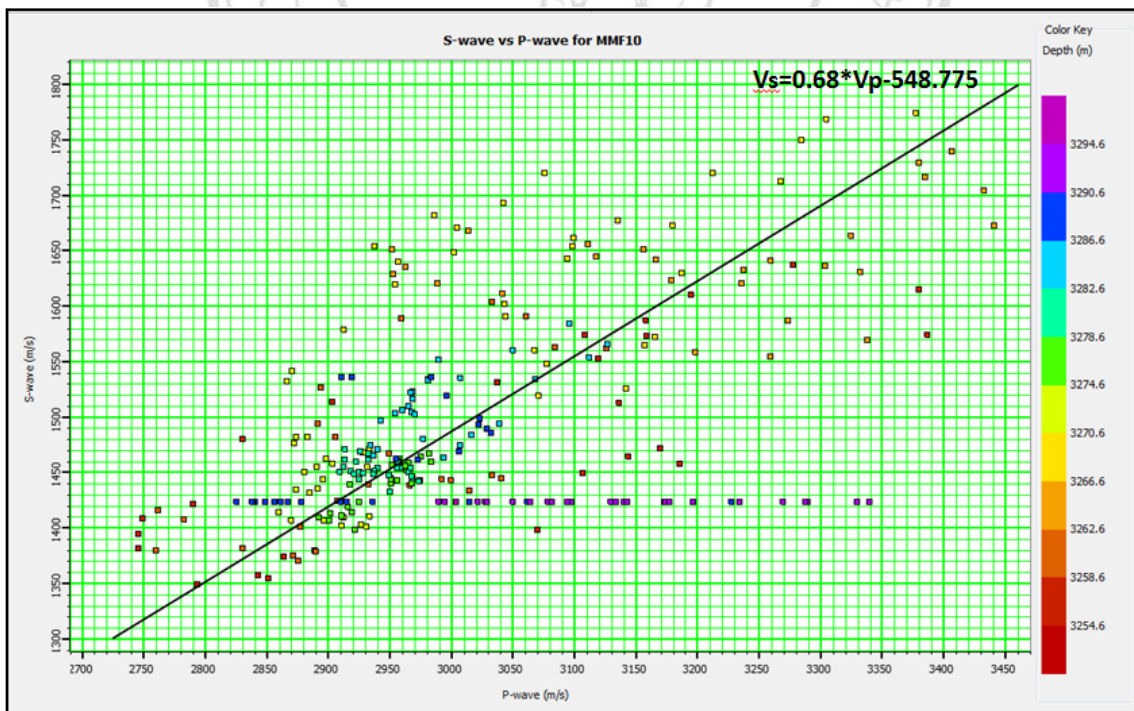


Figure 3.9: Cross plot V_s and V_p for MMF10. Linear relationship between V_s and V_p is defined by equation $V_s = 0.68 * V_p - 548.775$.

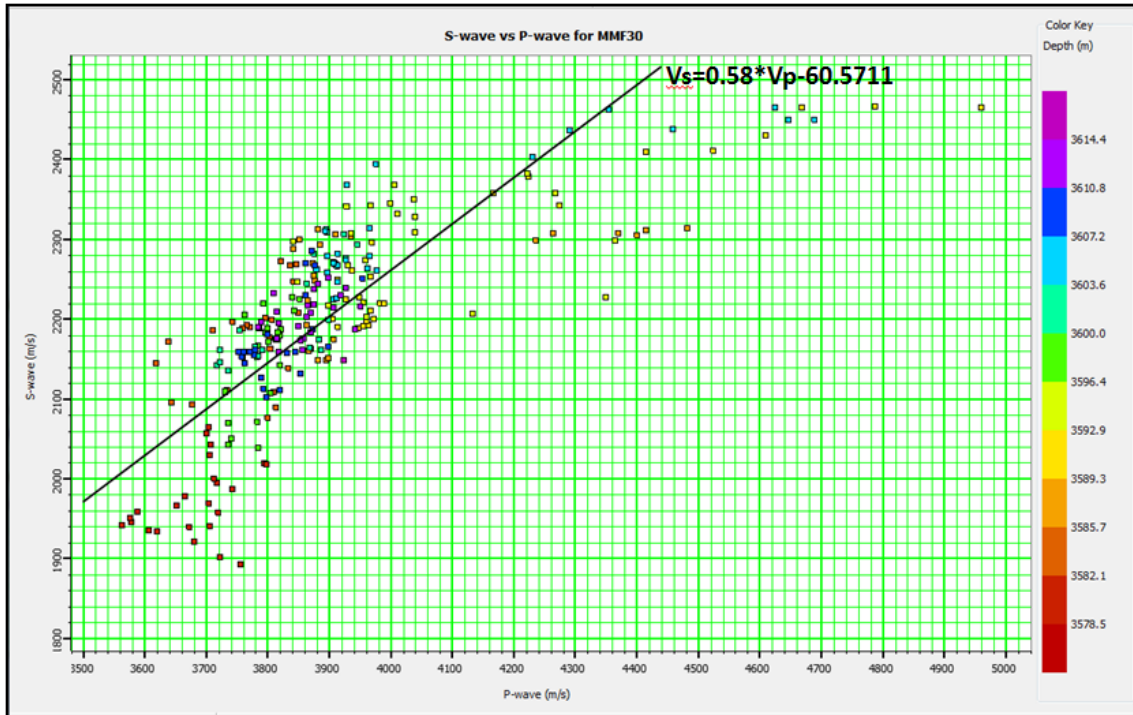


Figure 3.10: Cross plot V_s and V_p for MMF30. Linear relationship between V_s and V_p is defined by equation $V_s = 0.58 * V_p - 60.5711$.

The linear relationship between V_s and V_p above is used to generate predicted V_s for each interval. Next step is comparison between original V_s recorded at Well A, predicted V_s from localized relations for each interval and predicted V_s from Greenberg and Castagna empirical relation for sandstone using equation 3.1.

$$V_s = 0.8042 * V_p - 855.9, \quad (3.1)$$

where the units are in m/s. Three types of V_s for each interval are shown in Figures 3.11 to 3.13 while regression analysis comparisons are shown in Tables 3.2 to 3.4.

Copyright© by Chiang Mai University
All rights reserved

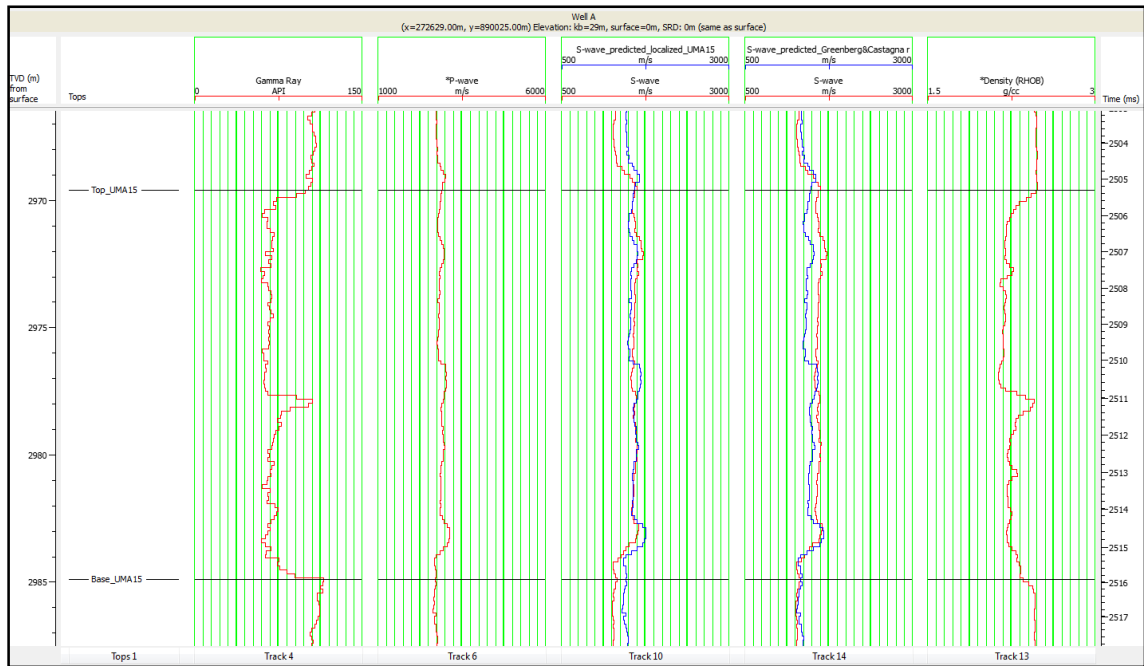


Figure 3.11: Plot of regression analysis for Vs prediction in UMA15 interval. Track 10 shows the recorded Vs in red and localized predicted Vs in blue while track 14 shows the recorded Vs in red and Greenberg and Castagna relation predicted Vs in blue.

Table 3.2: Comparison between Vs - Vp localized model and Greenberg and Castagna relation for UMA15 interval.

Depth	GR	Porosity	RHOB	Vp	Vs	Vs_predicted UMA15	Vs_Green & Castagna	Vs_diff predicted	prediction error	Vs_diff_Green & Castagna	Green&Castagna error
m	API	v/v	g/cc	m/s	m/s	m/s	m/s	m/s	%	m/s	%
2999	100	0.26	2.47	2892	1596	1580	1469	15	1	127	8
3000	63	0.23	2.27	2837	1555	1541	1424	14	1	131	8
3001	70	0.22	2.20	2863	1663	1559	1445	103	6	218	13
3002	66	0.22	2.21	2948	1637	1620	1513	17	1	123	8
3003	66	0.21	2.18	2827	1592	1534	1417	58	4	176	11
3004	68	0.22	2.19	2828	1600	1534	1417	65	4	183	11
3005	67	0.20	2.17	2775	1577	1497	1375	80	5	203	13
3006	63	0.20	2.15	3011	1588	1665	1564	-77	-5	24	2
3007	64	0.20	2.20	3015	1563	1668	1567	-105	-7	-4	0
3008	77	0.24	2.31	2894	1572	1582	1470	-9	-1	103	7
3009	71	0.22	2.23	2951	1610	1622	1515	-12	-1	94	6
3010	69	0.22	2.26	2887	1606	1576	1464	30	2	142	9
3011	68	0.22	2.22	2881	1578	1572	1460	5	0	118	7
3012	72	0.21	2.25	2915	1570	1596	1487	-26	-2	84	5
3013	60	0.23	2.21	3110	1606	1736	1644	-130	-8	-37	-2

In UMA15 interval from 2999.1 m to 3014.4 m (MD), the localized predicted Vs shows a better similar trend with the recorded Vs rather than Greenberg and Castagna relation predicted Vs. Table 3.2 shows the percentage error of the localized prediction Vs in comparison with Vs from recorded log from -8 % to 6 % meanwhile the percentage error of the Greenberg and Castagna relation prediction Vs from -2 % to 13 %. So, Vs from localized equation shows better accuracy than Greenberg and Castagna equation 3.1.

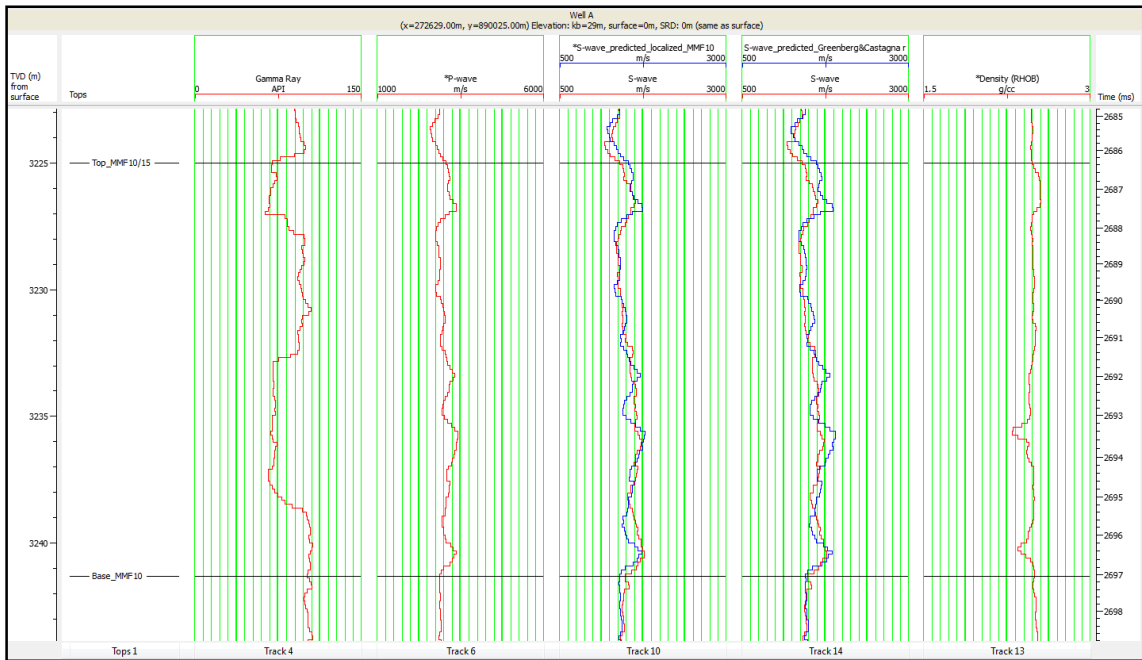


Figure 3.12: Plot of regression analysis for Vs prediction in MMF10 interval. Track 10 shows the recorded Vs in red and localized predicted Vs in blue while track 14 shows the recorded Vs in red and Greenberg and Castagna's relation predicted Vs in blue.

Table 3.3: Comparison between Vs - Vp localized model and Greenberg and Castagna relation for MMF10 interval.

Depth	GR	Porosity	RHOB	Vp	Vs	Vs_predicted MMF10	Vs_Green & Castagna	Vs_diff predicted	prediction error	Vs_diff_Green & Castagna	Green&Castagna error
m	API	v/v	g/cc	m/s	m/s	m/s	m/s	m/s	%	m/s	%
3255	74	0.21	2.54	3170	1473	1601	1692	-128	-9	-219	-15
3256	67	0.16	2.55	3195	1612	1618	1712	-6	0	-100	-6
3257	84	0.16	2.48	2831	1481	1371	1419	110	7	62	4
3258	96	0.27	2.49	2844	1358	1379	1429	-21	-2	-71	-5
3259	94	0.25	2.5	2877	1371	1402	1456	-30	-2	-84	-6
3260	100	0.28	2.49	2934	1441	1440	1502	1	0	-61	-4
3261	97	0.26	2.51	3000	1444	1486	1556	-41	-3	-111	-8
3262	93	0.24	2.49	3033	1606	1508	1582	98	6	24	1
3263	71	0.23	2.46	3339	1571	1715	1827	-144	-9	-256	-16
3264	73	0.22	2.46	2989	1622	1478	1547	144	9	75	5
3265	70	0.22	2.39	3238	1634	1647	1747	-13	-1	-113	-7
3266	72	0.22	2.43	3325	1665	1706	1817	-41	-2	-151	-9
3267	67	0.22	2.5	3099	1655	1553	1635	103	6	21	1
3268	81	0.23	2.5	3078	1549	1538	1618	11	1	-69	-4
3269	105	0.24	2.46	2987	1683	1476	1544	207	12	139	8
3270	104	0.2	2.38	3378	1776	1742	1859	34	2	-84	-5

In MMF10 interval from 3254.6 m to 3270.9 m (MD), the localized predicted Vs shows a better similar trend with the recorded Vs rather than Greenberg and Castagna predicted Vs. Table 3.3 shows the percentage errors of the localized prediction Vs in comparison with Vs from recorded log from -9 % to 12 % meanwhile the percentage error of the Greenberg and Castagna relation prediction Vs from -16 % to 8 %. So, Vs

from localized equation shows better accuracy than Greenberg and Castagna Equation 3.1.

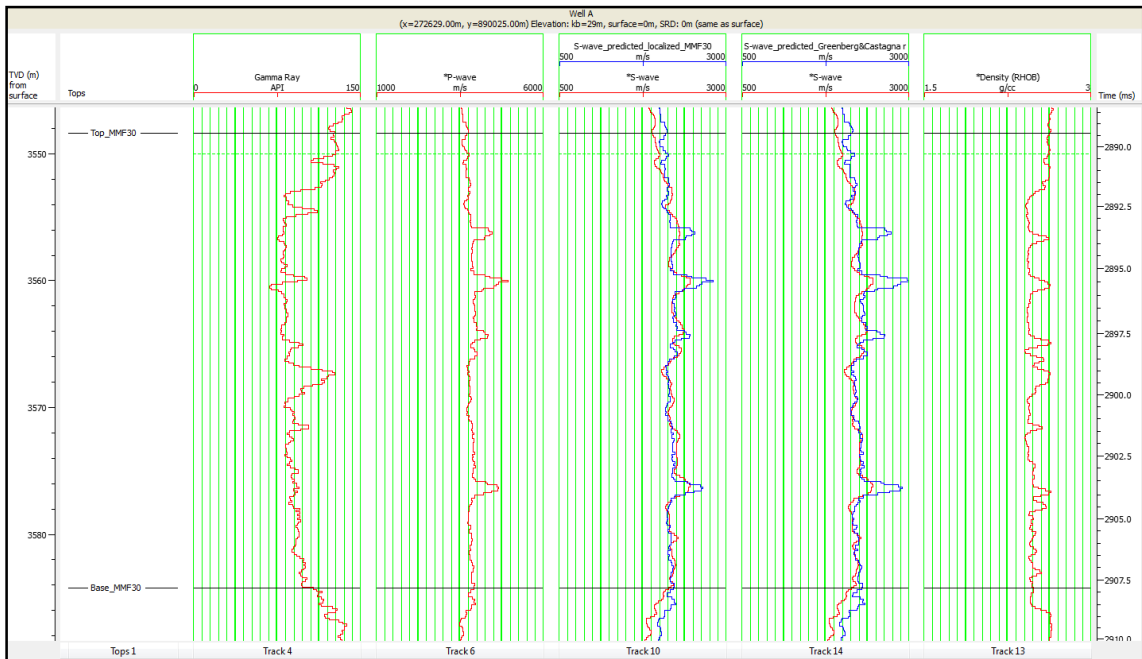


Figure 3.13: Plot of regression analysis for Vs prediction in MMF30 interval. Track 10 shows the recorded Vs in red and localized predicted Vs in blue while track 14 shows the recorded Vs in red and Greenberg and Castagna's relation predicted Vs in blue.

In MMF30 interval from 3578.5 m to 3614.4 m (MD), the localized predicted Vs shows a better similar trend with the recorded Vs rather than Greenberg and Castagna relation predicted Vs. Table 3.4 shows the percentage error of the localized prediction Vs in comparison with Vs from recorded log from -10 % to 6 % meanwhile the percentage error of the Greenberg and Castagna relation prediction Vs from -21 % to 5 %. So, Vs from localized equation shows better accuracy than Greenberg and Castagna Equation 3.1.

In summary, the percentage errors of 3 intervals (UMA15, MMF10 and MMF30) are compared to find the best linear equation for localized Vs prediction in the missing data interval. The percentage error of interval UMA15 have the lowest percentage error range, therefore it is chosen for prediction of Vs. The result of Vs after correction is shown in Figure 3.14. In conclusion, by using cross plots and statistical regression analysis the local Vs - Vp relationship suitable for the Nam Con Son Basin is derived and the missing values in the recorded shear wave velocities log are filled.

Table 3.4: Comparison between Vs - Vp localized model and Greenberg and Castagna relation for MMF30 interval.

Depth	GR	Porosity	RHOB	Vp	Vs	Vs_predicted MMF30	Vs_Green & Castagna	Vs_diff predicted	prediction error	Vs_diff_Green & Castagna	Green&Castagna error
m	API	v/v	g/cc	m/s	m/s	m/s	m/s	m/s	%	m/s	%
3579	124	0.19	2.61	3672	1942	2070	2095	-128	-7	-154	-8
3580	128	0.18	2.63	3717	1997	2095	2131	-98	-5	-134	-7
3581	127	0.18	2.63	3706	1943	2089	2123	-146	-8	-180	-9
3582	126	0.14	2.63	3704	2067	2088	2121	-21	-1	-54	-3
3583	96	0.16	2.54	3766	2195	2124	2171	71	3	24	1
3584	86	0.17	2.43	3638	2174	2050	2068	124	6	106	5
3585	92	0.16	2.43	3849	2210	2172	2237	38	2	-27	-1
3586	81	0.16	2.44	3852	2301	2174	2240	127	6	61	3
3587	77	0.10	2.58	3935	2305	2222	2307	83	4	-1	0
3588	81	0.16	2.43	3877	2250	2188	2260	61	3	-10	0
3589	85	0.15	2.44	3899	2153	2201	2277	-48	-2	-125	-6
3590	103	0.17	2.54	4789	2468	2717	2993	-249	-10	-524	-21
3591	76	0.12	2.53	4167	2361	2357	2493	4	0	-133	-6
3592	82	0.14	2.45	3947	2191	2229	2316	-38	-2	-125	-6
3593	85	0.16	2.44	3949	2230	2230	2318	0	0	-88	-4
3594	79	0.14	2.45	4005	2371	2263	2363	108	5	8	0
3595	86	0.09	2.62	3961	2205	2237	2327	-32	-1	-122	-6
3596	87	0.15	2.46	4040	2310	2283	2391	28	1	-80	-3
3597	95	0.15	2.48	3730	2111	2103	2142	8	0	-31	-1
3598	116	0.13	2.62	3820	2145	2155	2214	-10	0	-69	-3
3599	100	0.17	2.50	3817	2185	2154	2212	32	1	-26	-1
3600	83	0.16	2.45	3762	2208	2121	2167	87	4	41	2
3601	91	0.18	2.45	3778	2168	2131	2181	37	2	-13	-1
3602	97	0.15	2.52	3864	2246	2181	2249	66	3	-3	0
3603	86	0.15	2.42	3910	2270	2208	2287	63	3	-16	-1
3604	82	0.15	2.44	3879	2265	2190	2262	75	3	3	0
3605	92	0.14	2.49	3913	2249	2209	2289	39	2	-40	-2
3606	90	0.16	2.48	4291	2439	2429	2593	11	0	-153	-6
3607	91	0.07	2.62	4231	2405	2394	2545	11	0	-140	-6
3608	90	0.16	2.60	3797	2104	2142	2196	-38	-2	-92	-4
3609	94	0.17	2.49	3777	2157	2130	2180	26	1	-23	-1
3610	95	0.17	2.51	3799	2183	2143	2197	40	2	-14	-1
3611	92	0.17	2.46	3869	2186	2184	2254	2	0	-68	-3
3612	96	0.17	2.44	3814	2211	2152	2210	59	3	2	0
3613	100	0.17	2.51	3918	2232	2212	2293	20	1	-61	-3
3614	98	0.17	2.48	3871	2210	2185	2255	26	1	-44	-2

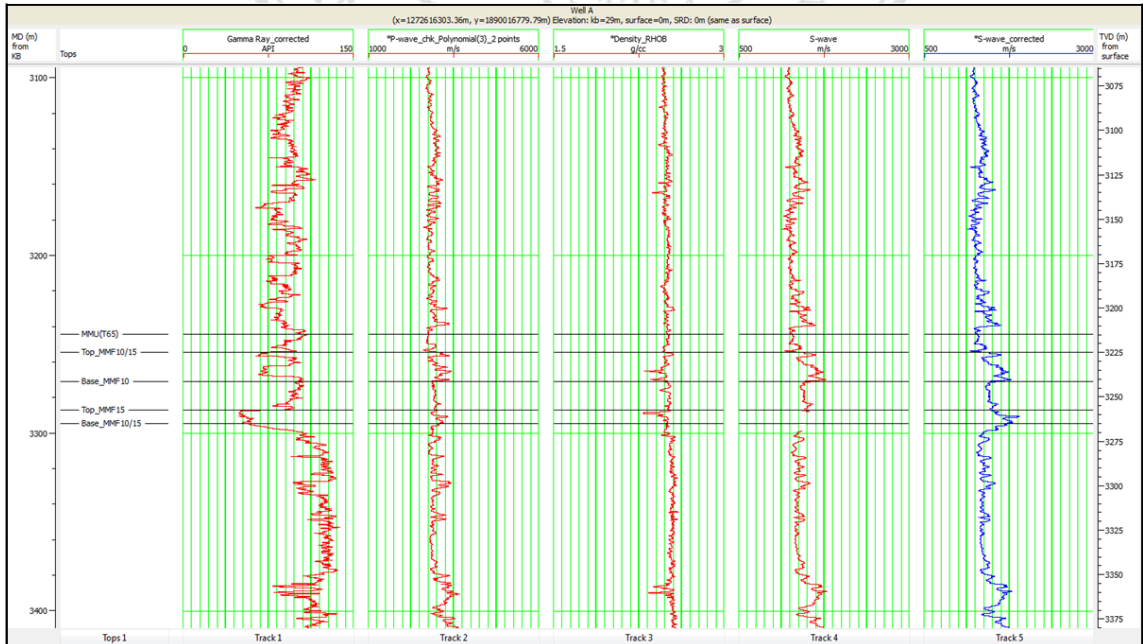
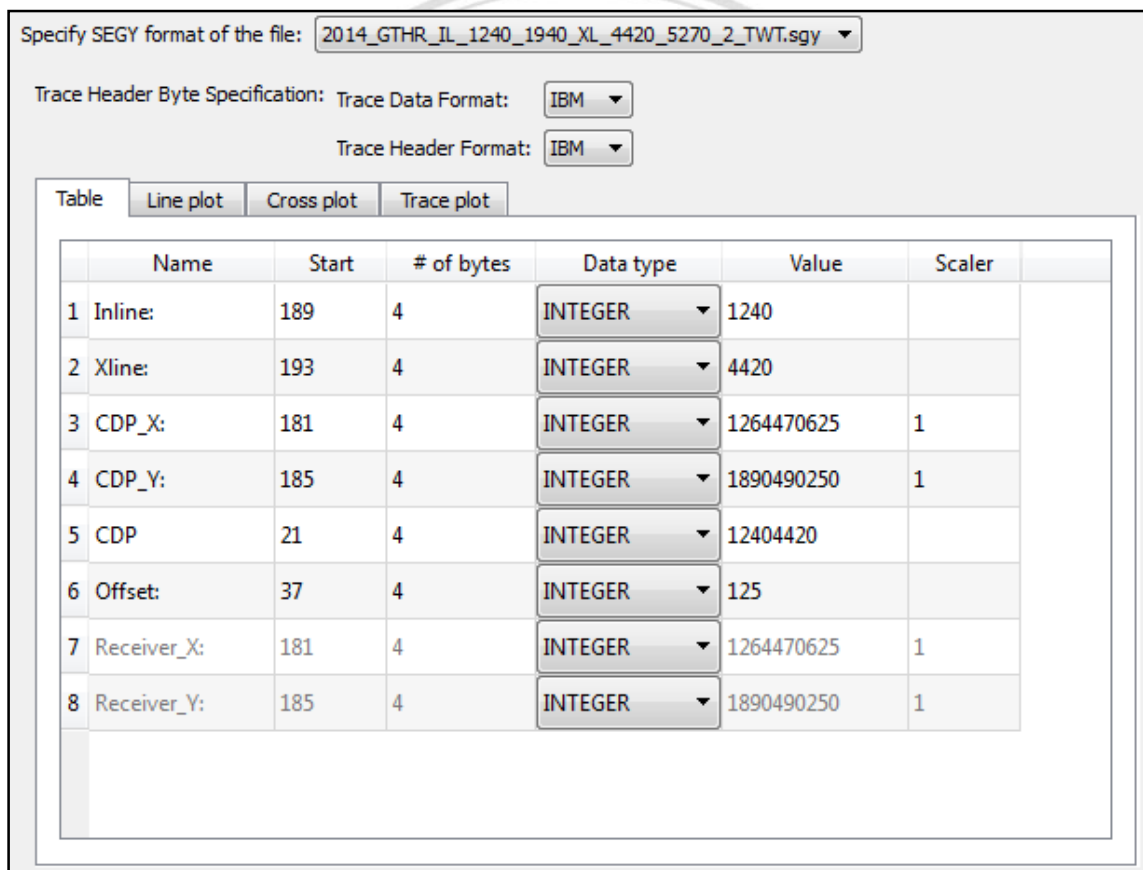


Figure 3.14: Plot of logs for well A. Track 4 shows the recorded Vs in red while track 5 shows the Vs after correction.

3.3 Seismic Data Enhancement

The first process is loading seismic volume into the Hampson Russell software for analysis and further processing. The most important point in loading data correctly is matching inline and cross-line byte locations parameters with the right values from the headers of seismic file (Figure 3.15). This seismic pre-stack data are processed by the company, the processing history is showed in Figure 3.16. Seismic data volume used in this study is migrated 3D seismic gathers (Figure 3.17).



Specify SEGY format of the file: 2014_GTHR_IL_1240_1940_XL_4420_5270_2_TWT.sgy

Trace Header Byte Specification: Trace Data Format: IBM

Trace Header Format: IBM

Table | Line plot | Cross plot | Trace plot

	Name	Start	# of bytes	Data type	Value	Scaler
1	Inline:	189	4	INTEGER	1240	
2	Xline:	193	4	INTEGER	4420	
3	CDP_X:	181	4	INTEGER	1264470625	1
4	CDP_Y:	185	4	INTEGER	1890490250	1
5	CDP	21	4	INTEGER	12404420	
6	Offset:	37	4	INTEGER	125	
7	Receiver_X:	181	4	INTEGER	1264470625	1
8	Receiver_Y:	185	4	INTEGER	1890490250	1

Figure 3.15: Inline and cross-line parameters from header of seismic volume.

```

C03 INLINE : 1401-1600, CROSSLINE: 1821-6185
C04 BIN GRID: 12.5x12.5M,TMAX:5000MS, SAMPLE RATE:4MS
C05 DATA : PSDM FINAL GATHER IN TIME
C08 PROCESSING HISTORY
C09 REFORMAT FROM FIELD TAPE (3592), SAMPLE RATE:2MS
C10 TRACE EDITS FROM OBSERVERS LOG
C11 SYSTEM DELAY CORRECTIONS: -120 MS
C12 NAV & SEIS MERGE, LOW CUT FILTER:3 Hz
C13 ANTI-ALIAS FILTER:110 HZ, RESAMPLE 2MS TO 4MS
C14 SWELL NOISE ATTENUATION, LINEAR NOISE ATTENUATION
C15 TIDAL STATICS, SHALLOW WATER DE-MULTIPLE (SWD)
C16 2D SURFACE RELATED MULTIPLE ATTENUATION (SRME)
C17 TAU-P DECONVOLUTION
C18 ALTERNATE TRACE DROP WITH K-FILTER TO BIN SIZE:12.5x25M
C19 NORMAL MOVEOUT CORRECTION (NMO)
C20 HI-RESOLUTION 2D RADON DEMULTIPLE
C21 QCOMP-PHASE ONLY, Q=130, FREQ-NYQUIST
C22 3D MISSING TRACE INTERPOLATION (RALFT3D)
C23 RANDOM NOISE ATTENUATION
C24 TRACE INTERPOLATION TO 12.5X12.5M GRID
C25 REVERSE NMO, REMOVE SPH DIV
C26 Q-HFCBM WITH FINAL MODEL, HALF-APERTURE 4.5KM
C27 RADON DEMULTIPLE
C28 GAMMA RESIDUAL MOVEOUT CORRECTION (GRMO)
C29 3D CDP FLATTENING (FLAT3D), SHALLOW DEMULTIPLE

```

Figure 3.16: Processing history of seismic volume.

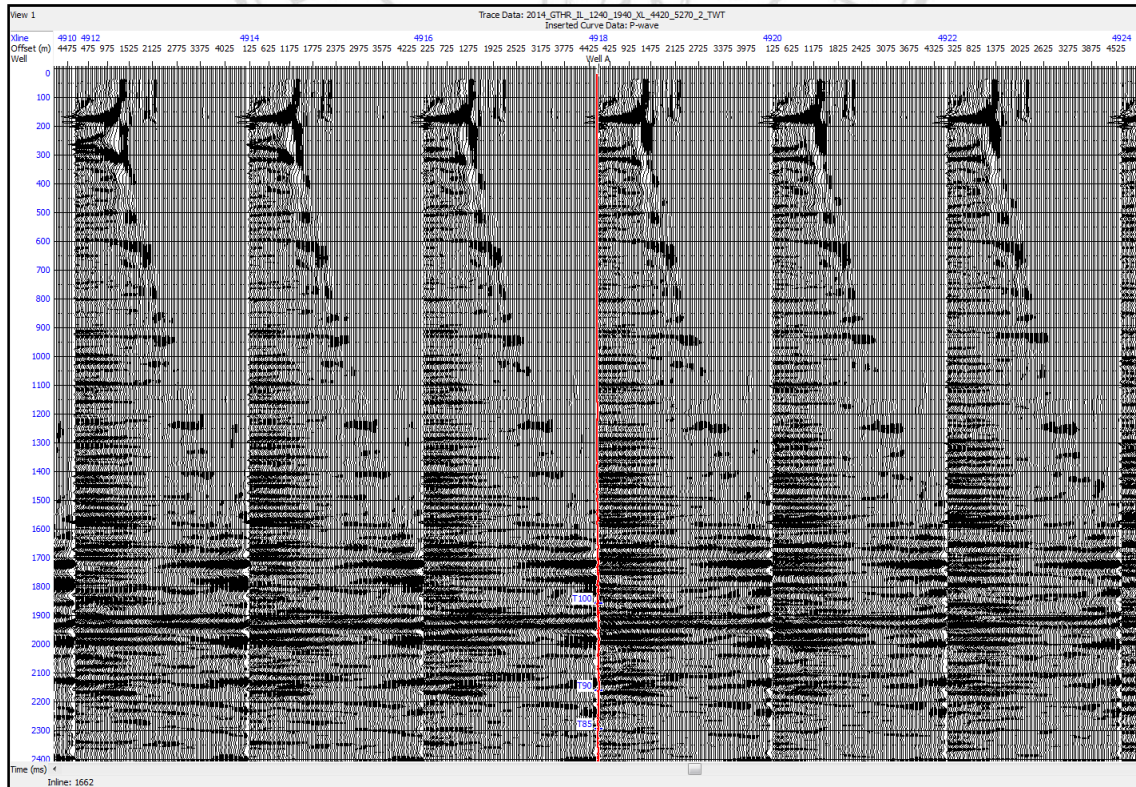


Figure 3.17: 3D migrated seismic gathers.

The results of pre-stack seismic inversion are ultimately dependent on the quality of the input seismic data. Good result is produced when the seismic data is rich in frequencies which contain both high and low frequencies, relatively free of noise, high and consistent amplitude, and the signal events are aligned. Although seismic data are good processed but some problems still present in 3D NMO-corrected seismic gathers. These problems such as overcorrected and under-corrected reflection after NMO correction or random noises can be visually detected in seismic gathers. To obtain a flattening of reflections, the velocity must have the correct value. When the velocity is too low, the reflection is overcorrected and the reflection curves upwards. When the velocity is too high, the reflection is under-corrected and the reflection curves downwards.

Therefore, conditioning of gathers in Hampson Russell software is carried out to enhance the input seismic data. Seismic data conditioning is a key improvement for any quantitative seismic interpretation or reservoir characterization project using pre-stack seismic inversion technology. Because the seismic dataset in this study had been already processed, the reflections are flat in the seismic gathers, however there are still high frequency traces after NMO correction. After considering seismic data carefully, two steps of pre-stack seismic processing are applied in order to improve S/N ratios, enhance amplitude, bandwidth.

3.3.1 Mute

The first step applying for gathers conditioning is mute. In pre-stack processing workflow, mute function is applied in CMP domain after NMO correction to remove unwanted direct arrivals, refractions and NMO stretch. In Hampson Russell software, the mute option applies an offset dependent mute to a range of gathers. It removes faulty data from a set of gathers by setting the amplitude for these data to zero, so only the reliable data are used for the seismic gathers. In this dataset, mute is applied mainly to remove the effect of NMO stretch due to low frequency wavelet at the far offset after NMO correction. Besides, muting can also compensate for other errors like refractions and noises at the far offsets. Result of the seismic gathers after muting shows better image of seismic gathers with no stretching reflection (Figure 3.18).

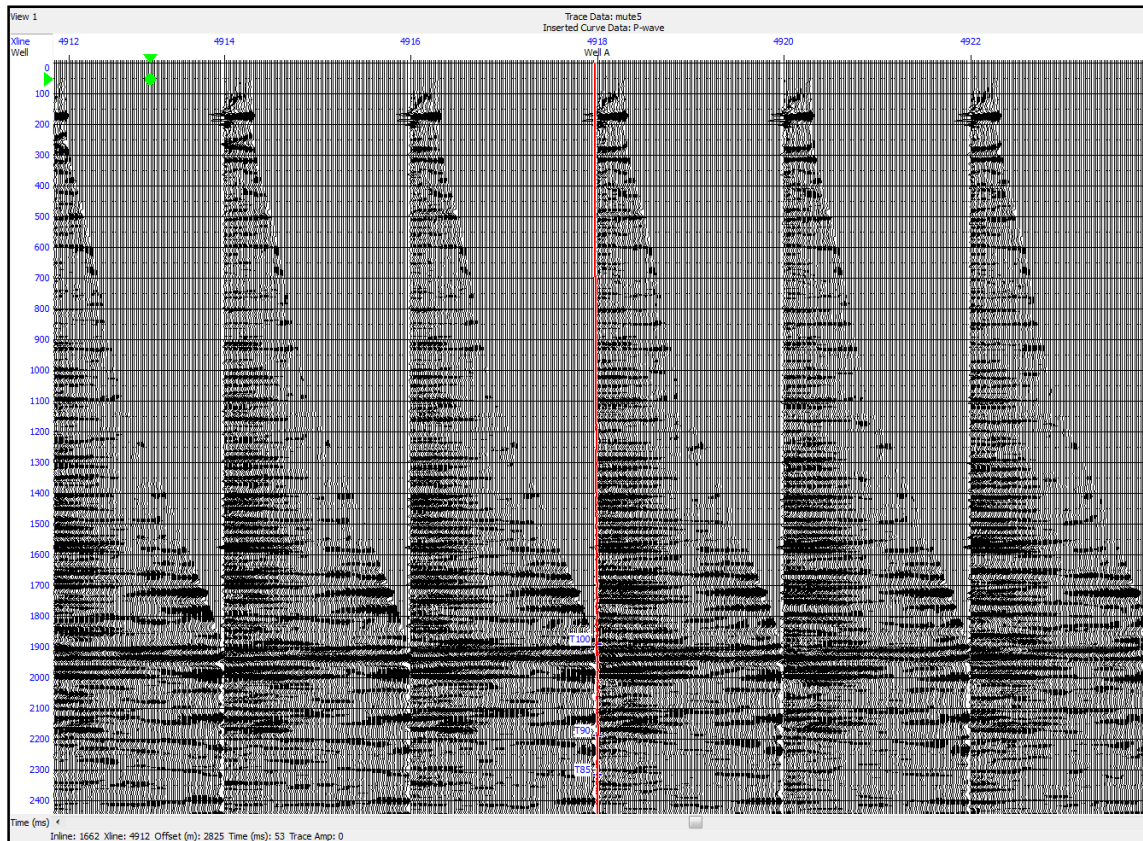


Figure 3.18: Seismic offset gathers after applying mute.

3.3.2 Super Gather

The second step of conditioning seismic dataset is generating super gather. Meaning of super gather firstly is discussed by Ostrander (1984), a method of partial summing seismic traces. From Ostrander (1984), to form partial summing traces, all traces fall within boxes which are 5 CDPs by 4 offsets in dimension and which are summed together forming a single output trace. Same process happens in the software, the super gather process analyzes a subset of seismic gathers, and calculates a number of “super-gathers”, in which each trace represents a range of offsets. CDPs will be averaged by collecting adjacent CDPs and add them together. By creating the super gathers, S/N ratio is enhancement and random noises are also been eliminated. For this dataset, the super gathers are created by rolling window of 5 in both inline and cross-line, that means 5 CDPs bin locations are averaged. In the output bin, each gather has 90 offset bins ranging from 125 m to 4575 m. The number of bins in the output super gathers is kept as 90 folds of the original data set in order to keep the stratigraphic features in seismic data. It is obvious that the S/N ratio at interest zone from 2400 ms to 3000 ms

was improved. The comparison between before and after creating seismic super gathers is shown in Figure 3.19. Red dashed lines represent examples of zones where effects of noise are reduced. It is obvious that the reflections look sharper and some random noises have been removed. Figure 3.20 show the super gathers at the Well A location.

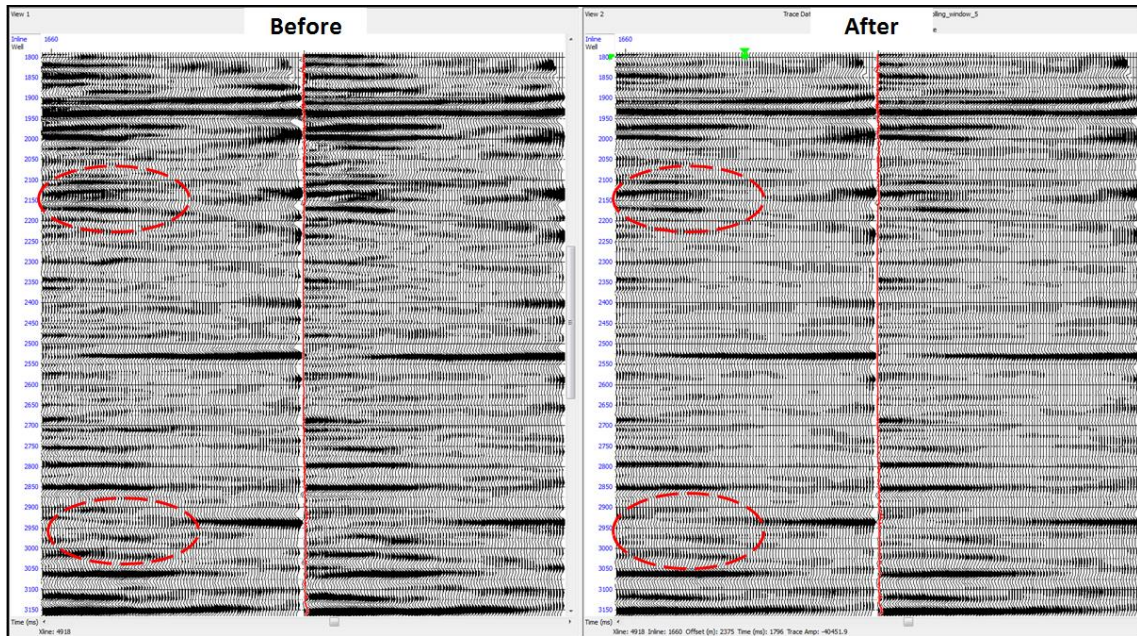


Figure 3.19: Before and after creating seismic super gathers. Red dashed lines represent examples of zones where effects of noise are reduced.

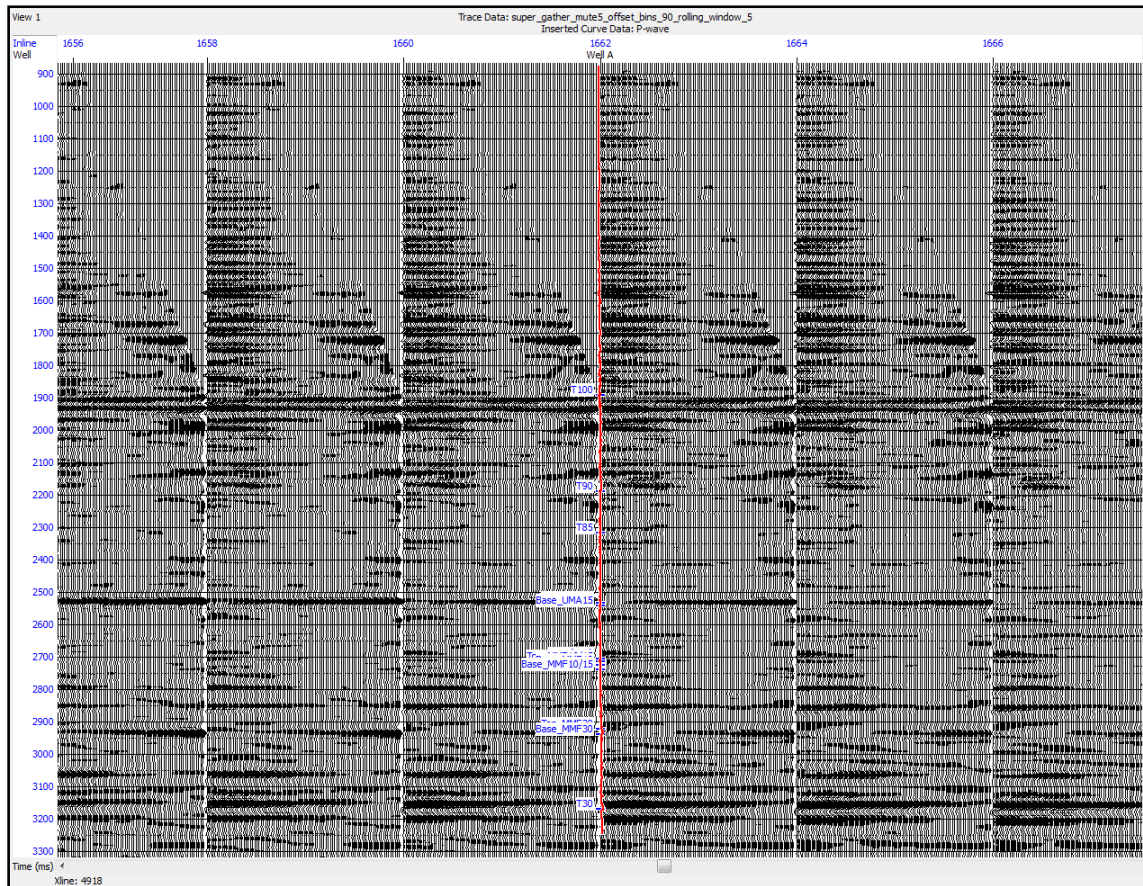


Figure 3.20: Super gathers at well location from zone of interest.

3.3.3 Angle Gather

Elastic impedance (EI) is generalization of acoustic impedance for variable incidence angle (Connolly, 1999). Therefore, the range of angle of incidence needs to be determined at the interest interval to do elastic impedance inversion. The incident angles are displayed in colors on the super gather plot to decide what range of angles to generate angle stacks (Figure 3.21). The super gather is offset dependent so to transform it to the angle gather a velocity model is used. Hampson Russell software has many choices to specify the velocity model, for a big volume like this, the velocity volume which provided by company is used. The velocity volume is in root mean square (RMS) velocity which will be transformed to interval velocity automatically by the Hampson Russell software. Vertical smoother value for the RMS velocity is 500 ms.

The maximum incident angle at the interest interval (2400 ms to 3000 ms) is approximately 40 degrees in the incident angle colors display. The angle gather is displayed in Figure 3.22. The created angle gather volume is full angles 40 degrees

gather, it will be used later to generate near, mid and far angle stack for elastic impedance inversion.

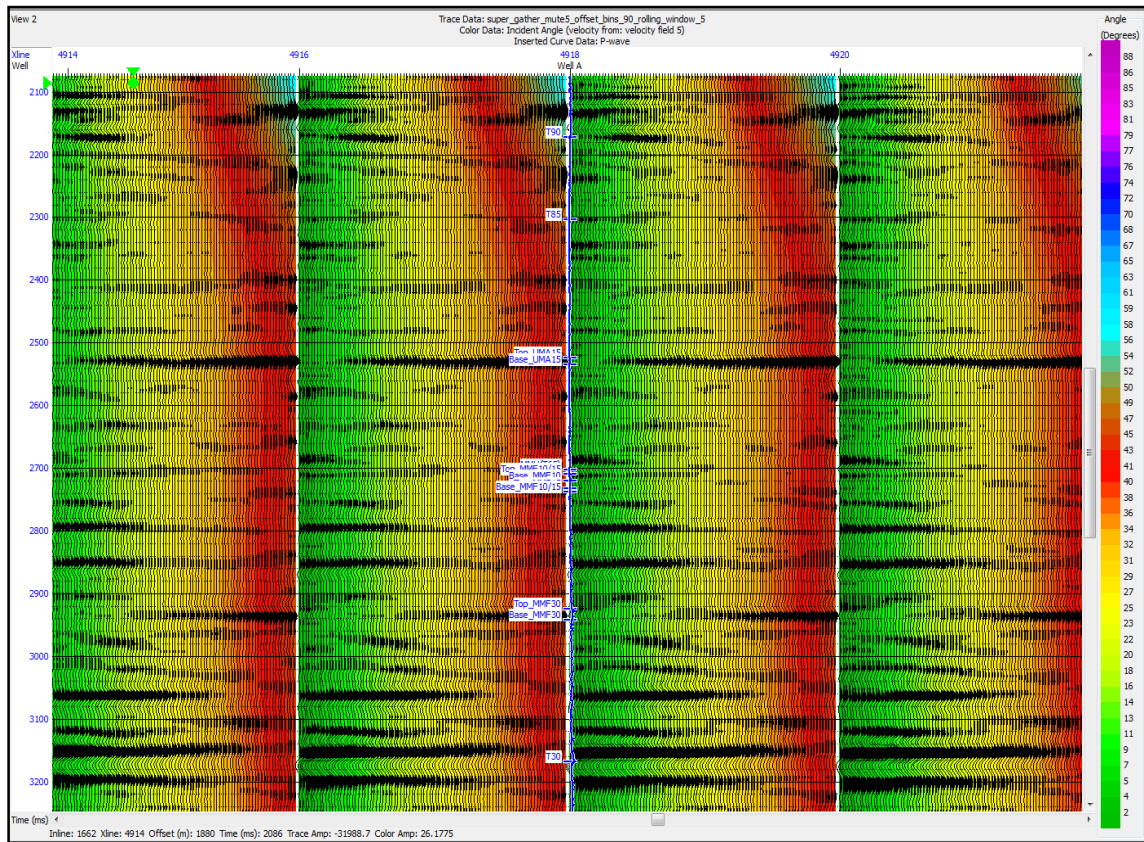


Figure 3.21: The incident angles are displayed on super gather plot.

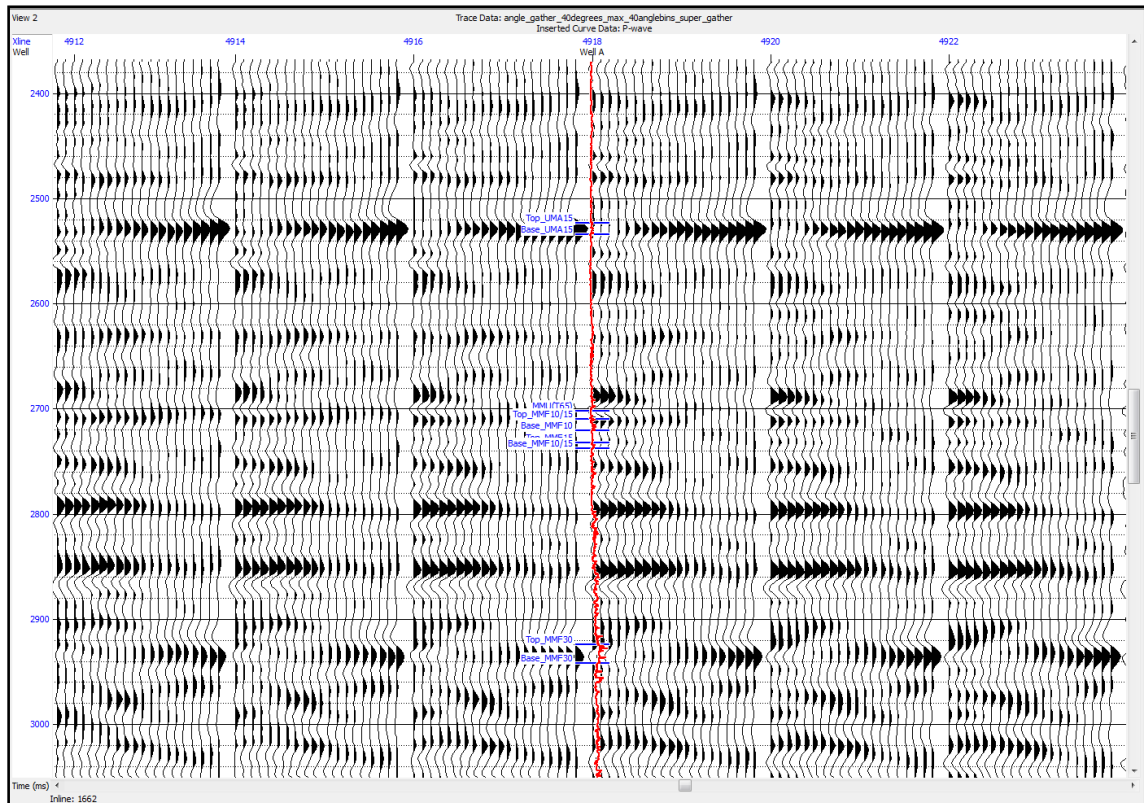


Figure 3.22: Angle gather (40 degrees) at the interest interval.

3.3.4 CDP Stack

The CDP stack is created by using all 162,306 CDPs super gather with time window from 0 to 5000 ms and offset range from 150 m to 4550 m by one bin trace. The reservoir interval UMA15 is clearly observed due to high anomaly amplitude at around 2510 ms meanwhile the reservoir interval MMF30 is still observed with lower amplitude anomaly at 2930 ms. The CDP stack volume (Figure 3.23) will be used in the other later processes.

Copyright © by Chiang Mai University
All rights reserved

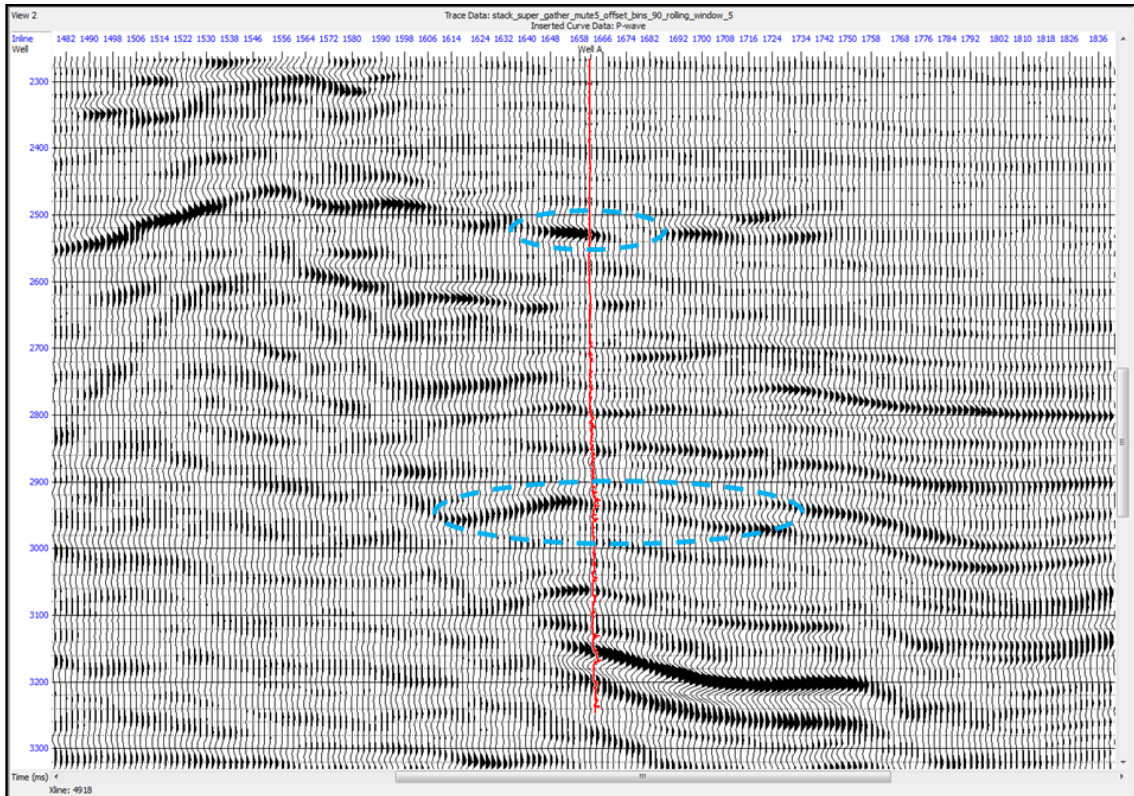


Figure 3.23: CDP super gather stack shows zone of interest. Two oval dashed blue lines show two reservoir intervals UMA15 and MMF30.